Catalysis Communications 36 (2013) 31–37

Contents lists available at SciVerse ScienceDirect

Catalysis Communications

journal homepage: www.elsevier.com/locate/catcom

Short Communication

Sulfonated rice husk ash (RHA-SO_3H): A highly powerful and efficient solid acid catalyst for the chemoselective preparation and deprotection of 1,1-diacetates

Farhad Shirini *, Manouchehr Mamaghani, Mohadeseh Seddighi

Department of Chemistry, College of Science, University of Guilan, Rasht, zip code: 41335, Post Box: 1914, Islamic Republic of Iran

ARTICLE INFO

Article history:
Received 2 January 2013
Received in revised form 21 February 2013
Accepted 25 February 2013
Available online 4 March 2013

Keywords:
Rice husk ash
Sulfonated rice husk ash
Solid acid
Protection
Solvent-free condition
1,1-Diacetates

ABSTRACT

Rice husk ash (RHA), as a source of amorphous silica, was treated with chlorosulfonic acid and sulfonated rice husk ash (RHA-SO_3H) as a highly powerful solid acid catalyst was obtained and characterized with a variety of techniques including IR, TGA, SEM, XRD, pH analysis, Hammett acidity function and BET method. This solid acid showed excellent catalytic activity for the protection and deprotection of aldehydes with Ac_2O at room temperature under solvent free conditions. The procedure gave the products in excellent yields in very short reaction times and good to high yields. Also this catalyst can be reused for several times without loss of its catalytic activity.

1. Introduction

Protection and deprotection of functional groups are often necessary during a multistep organic synthesis in order to obtain chemoselectivity. Aldehydes are often present in organic molecules so development of economical, efficient and mild procedures for the protection of them is very important for synthetic organic chemistry. Among various procedures for protection of aldehyde, preparation of 1,1-diacetates from the reaction of aldehydes and acetic anhydride is the most common route due to the stability of the products in the neutral and basic conditions [1,2]. 1,1-Diacetates are also important for the preparation of other compounds, for example in reaction with appropriate nucleophiles they can be converted to other useful functional groups [3]. On the other hand α,β-unsaturated diacetates are important starting materials for Diels–Alder reactions [4]. A variety of catalysts including $FeCl_3$ [2], sulfuric acid [5], Zn-montmorillonite [6], $Bi(NO_3)_3 \cdot 5H_2O$ [7], $In(OTf)_3$ [8], P_2O_5/Al_2O [9], $CuSO_4 \cdot 5H_2O$ [10], Silica sulfuric acid [11], $HClO_4$-SiO_2 [12], $Al(HSO_4)_3$ [13], SO_4^{2-}/SnO_2 [14], [Hmim]HSO_4 [15] and [bmpy]HSO_4 ionic liquid [16], silica-bonded S-sulfonic acid [17], saccharin sulfonic acid [18], *N*-sulfonic acid poly(4-vinylpyridinium) chloride [19], ZSM-5-SO_3H [20] have been reported for the promotion of the acetylation of aldehydes with acetic anhydride. Although these methods are an improvement, most of them suffer from disadvantages such as long reaction times, need of organic solvents, expensive catalyst, use of excess amounts of the acylating agents, harsh reaction conditions and non-recoverability of the catalyst. Therefore, introduction of efficient and economical catalysts that solve these drawbacks is desirable.

Replacement of conventional, toxic and polluting Bronsted and Lewis acid catalysts with eco-friendly reusable heterogeneous catalysts is an area of current interest. In this context, there has been renewed interest in the synthesis of solid acid catalysts for organic reactions. Solid acid catalysts have many advantages compared to traditional liquid acids such as their efficiency, operational simplicity, easy recyclability and recoverability, non-corrosive nature and friendly to the environment, all factors which are important in industry. Therefore, solid acid catalysts can play a significant role in the development of clean technologies. Among various supports that can be used for the preparation of the above mentioned catalysts (silica, montmorillonite, organic polymer and zeolite), silica is one of the more extensively used cases, because it has many advantages such as ease of handling, commercially available, low cost, high mechanical and thermal stability and non-corrosiveness.

Recently utilization of waste materials has been found to be of increasing interest. Rice husk, the outer covering of rice grains obtained during the milling process, is one of the main agricultural residues. It mainly consists of cellulose, hemicelluloses, lignin, silica and minor other mineral composition [21]. Societies often dispose of the rice husk waste using open burning that leads to environmental pollution and damages to the land and the surrounding area in which it was dumped. In recent years, the application of rice husk as an energy

---

* Corresponding author. Tel./fax: +98 131 3233262.
E-mail address: shirini@guilan.ac.ir (F. Shirini).

1566-7367/$ – see front matter © 2013 Elsevier B.V. All rights reserved.
http://dx.doi.org/10.1016/j.catcom.2013.02.022

source for biomass power plants, rice mills and brick factories is increasing due to its high calorific power [22]. In this combustion, rice husk ash (RHA) is produced. RHA possesses excellent pozzolanic activity due to its high surface area and high silica content [23,24], so it is used in cement, concrete and white ware production and the preparation of lightweight aggregate [25,26]. Also, it has been employed as adsorbent for heavy metals, purifying biodiesel and producing zeolites and silica powders [27–29]. Although useful, the reported method for the preparation of pure silica from rice husk ash needs various stages and a long time [29]. On the basis of these points it can be concluded that, at the same conditions, the use of RHA as a support for the preparation of catalysts is better than the use of silica which is prepared via precipitation method during various stages and long time.

2. Experimental

2.1. Instrumentation

The ^{1}H NMR (400 MHz) and ^{13}C NMR (100 MHz) were run on a Bruker Avance DPX-400 FT-NMR spectrometer (δ in ppm). The chemical composition of RHA was analyzed using X-ray fluorescence (XRF) spectrometer (Model Magix Pro, Philips). The FT-IR spectra were run on a VERTEX 70 Brucker company (Germany). Thermogravimetric analyses (TGA) were performed on Polymer Laboratories PL–TGA thermal analysis instrument (England). Samples were heated from 25 to 600 °C at ramp 10 °C/min under N_2 atm. The adsorption–desorption isotherms and the specific surface area (S_{BET}) were determined from nitrogen adsorption studies using Micro neotype StarII system. Scanning electron microphotographs (SEM) were obtained on a SEM-Philips XL30. X-ray diffraction (XRD) measurements were performed at room temperature on diffractometer Model XRD 6000, PHILIPS Xpert pro using Co–Kα radiation (K = 1.7890 Å) with the beam voltage and a beam current of 40 kV and 30 mA, respectively.

2.2. Preparation and chemical composition of RHA

The rice husk sample was obtained from an Iranian type of rice, named as Hassani. It was burned at 600 °C for 1 h to obtain RHA. The X-ray fluorescence (XRF) analysis showed a high value of silica content for the sample (up to 80%). Other composition such as Al_2O_3, Fe_2O_3, SO_3, P_2O_5, K_2O, Na_2O and CaO are also present in RHA as a very small proportion of metallic elements (Table 1).

2.3. Catalyst preparation (RHA-SO_3H)

A 50 mL suction flask charged with 3.0 g of RHA and 10 mL $CHCl_3$, was equipped with a constant-pressure dropping funnel containing chlorosulfonic acid (0.7 mL) and a gas inlet tube for conducting HCl gas into water as an adsorbing solution. Chlorosulfonic acid was added drop wise over a period of 20 min while the reaction mixture was stirred in an ice bath (0 °C). After addition was completed the mixture was stirred for an additional 2 h at room temperature to remove HCl. Then, the mixture was filtered and the filtrate was washed with methanol (20 mL) to remove the remaining HCl and the solid residue was dried at 70 °C for 1 h to afford RHA-SO_3H (3.6 g) as an earthy powder (Scheme 1).

Table 1
Chemical composition of RHA conducted by X-ray fluorescence analysis (wt%).

SiO_2	Al_2O_3	Fe_2O_3	SO_3	P_2O_5	K_2O	Na_2O	CaO	Cl	LOI[a]
80.82	0.25	0.38	0.39	0.44	1.25	0.96	0.82	1.99	12.70

[a] Loss on ignition.

Scheme 1. Preparation of the catalyst (RHA-SO3H) catalyzed by RHA-SO3H.

2.4. General procedure for the preparation of 1,1-diacetate

Aldehyde (1 mmol) was added to a mixture of RHA-SO_3H (10 mg) and acetic anhydride (1.5 mmol) and the resulting mixture was stirred at room temperature. After completion of the reaction (monitored by TLC), dichloromethane (20 mL) was added and the catalyst was separated by filtration. The organic phase was washed with 10% aqueous solution of sodium bicarbonate (2 × 20 mL) and dried over Na_2SO_4. The solvent was removed under reduced pressure to afford the desired product. The solid crude product was purified by recrystallization from cyclohexane. The spectral (IR, ^{1}H and ^{13}C NMR) data of fluorene-3-carbaldehyde as a new compound is presented below:

Table 3, Entry 20: IR (neat) $\nu = 1765\ \text{cm}^{-1}$; ^{1}H NMR ($CDCl_3$, 400 MHz): $\delta = 2.17$ (s, 6H, CH_3), 2.95 (S, 2H, CH_2), 7.35–7.84 (m, 8H, ArH, CH) ppm; ^{13}C NMR ($CDCl_3$, 100 MHz): $\delta = 20.9$, 36.9, 90.1, 119.9, 120.2, 123.4, 125.1, 125.5, 126.9, 127.2, 133.7, 140.9, 143.3, 143.5, 143.6, 168.9 ppm.

2.5. General procedure for the deprotection of 1,1-diacetates

A mixture of 1,1-diacetate (1 mmol), RHA-SO_3H (30 mg) in acetonitrile (2 mL) was stirred vigorously at 60 °C. After completion of the reaction (monitored by TLC), the organic solvent was evaporated. Then the reaction mixture was diluted by ethyl acetate (20 mL) and filtered to separate the catalyst. The organic phase was washed with 10% aqueous solution of sodium bicarbonate (2 × 10 mL) to remove excess of Ac_2O and dried over Na_2SO_4. The solvent was evaporated under reduced pressure. The resultant product was passed through a short column of silica gel (n-hexane-EtOAc, 9:1) to afford the pure aldehyde.

3. Results and discussion

3.1. Catalyst characterization

3.1.1. FT-IR analysis

The infrared spectra of RHA and RHA-SO_3H are shown in Fig. 1. In the case of RHA, the peaks at 3460 and 1640 cm ^{1} are respectively

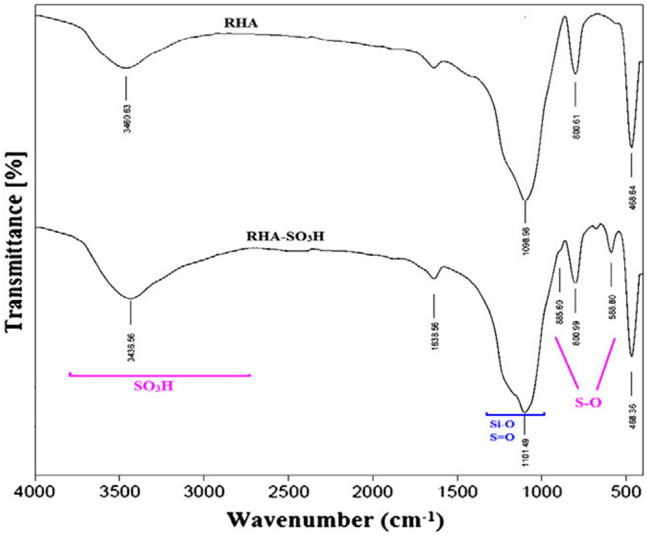

Fig. 1. FT-IR spectra of RHA and RHA-SO_3H.

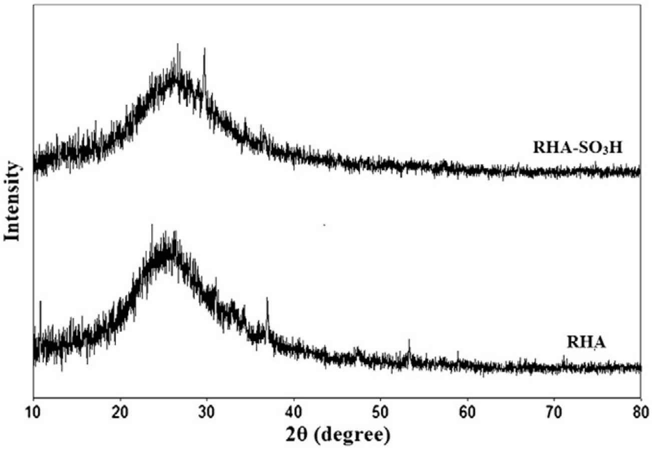

Fig. 2. XRD patterns of RHA in comparison with RHA-SO_3H.

attributed to the stretching and bending modes of the SiOH groups and the adsorbed water. The strong peaks at 1100, 801 and 468 cm^{-1} are assigned to asymmetric stretching, symmetric stretching and bending modes of SiO_2, respectively [29].

The RHA-SO_3H is also characterized. The broad band around 1100 cm^{-1} is assigned to stretching modes of Si–O and S=O bands which are overlapped together. The bands in 588 and 855 cm^{-1} correspond to the S–O stretching vibrations. The spectrum also shows a relatively broad band around 2700 to 3600 cm^{-1} due to OH stretching absorption of the SO_3H group [30].

3.1.2. Powder X-ray diffraction

Fig. 2. represents the X-ray diffraction (XRD) patterns of the RHA and RHA-SO_3H. As can be seen in the RHA pattern, a broad peak appeared around 2θ equal to 26° clearly indicated that silica of rice husk ash was mainly in the amorphous form [31]. The peak intensities of RHA-SO_3H are remained almost unchanged compared to RHA pattern that indicate an ordered mesoporosity of the supports even after modification.

3.1.3. Thermal analysis

The thermal stability of RHA and RHA-SO_3H was determined by Thermogravimetric analysis (TGA) and differential thermogravimetry (DTG) curves, as shown in Fig. 3. The results indicate that RHA showed a weight change below 100 °C due to the loss of the physically adsorbed water and then had a steady weight loss at the temperature lower than 600 °C, which could be ascribed to the loss of terminal groups such as –OH terminal groups [32].

The TGA and DTG analysis of RHA-SO_3H show two-stage decomposition, completely different from RHA. The first weight loss below 100 °C can be due to desorption of water and the second weight loss started at 170 °C can be attributed to the decomposition of covalently bounded –SO_3H groups [30]. These results indicate that the catalyst is stable up to around 170 °C. It is important to note that, on the basis of Fig. 3 (b and c), it can be concluded that the grafted –SO_3H groups increase the tendency of the absorption of water on the surface of the catalyst.

3.1.4. Surface area and pore distribution measurements

N_2 adsorption–desorption measurements (BET and BJH methods), which have been a powerful tool for nano- or mesoporous material characterization, were performed to obtain more insights into the modified porous silica materials. The N_2 adsorption–desorption isotherm of RHA and RHA-SO_3H (Fig. 4a) showed that both samples exhibited type IV isotherms according to the literature, which indicates that the samples are mesoporous materials. Furthermore, the hysteresis loop of both samples showed H3 categories, which should be a result of

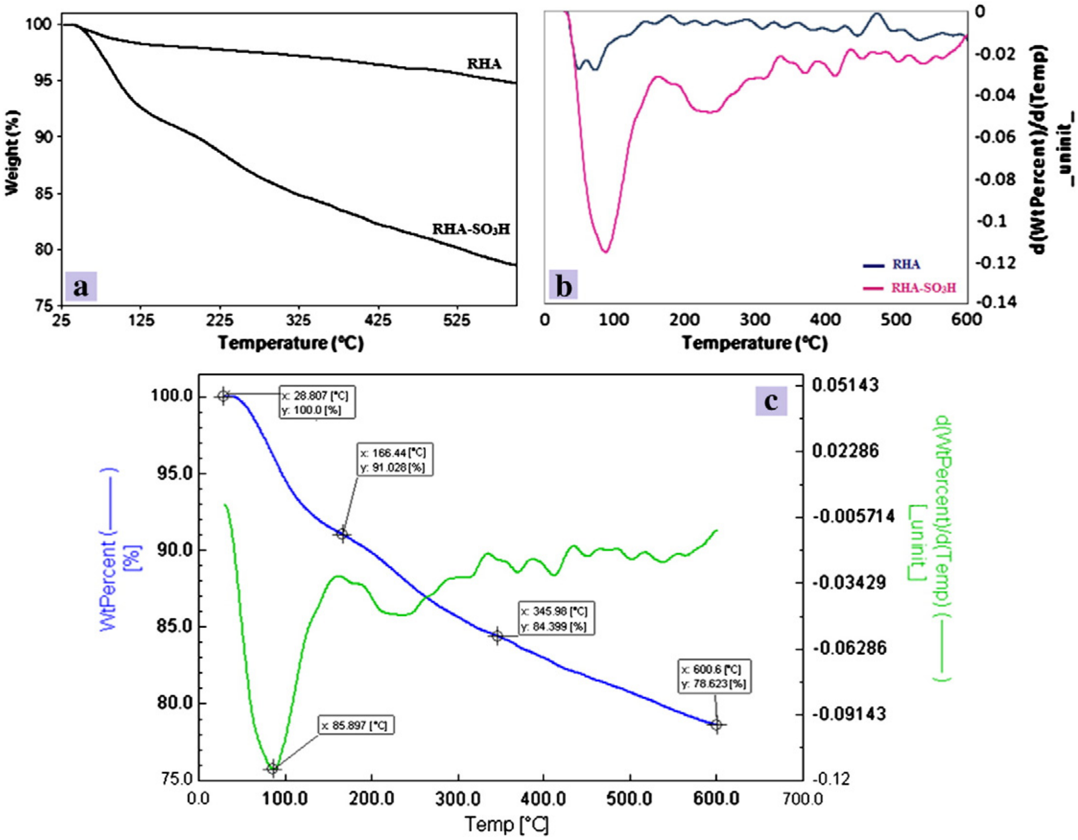

Fig. 3. (a) TGA curves of RHA and RHA-SO_3H, (b) DTG curves of RHA and RHA-SO_3H and (c) TGA–DTG curve of RHA-SO_3H.

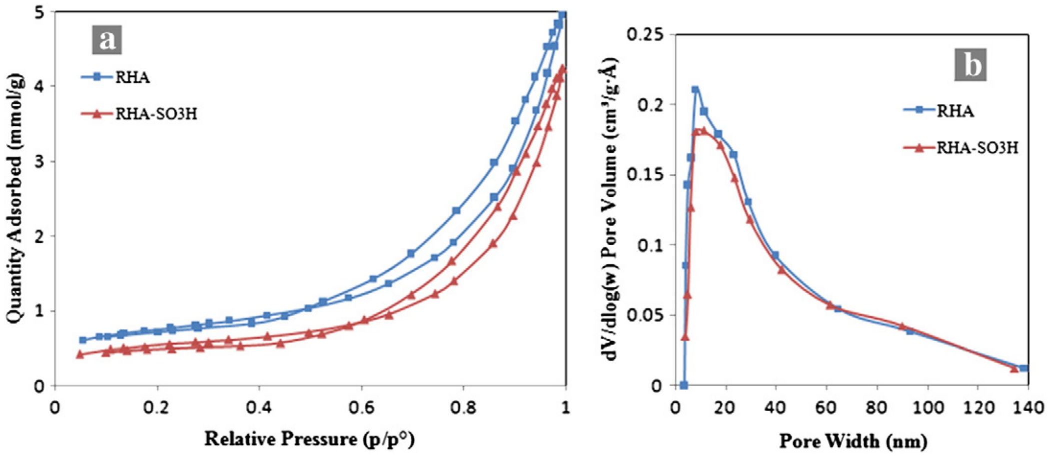

Fig. 4. The N_2 adsorption–desorption isotherm (a), and pore size distribution (b) of RHA and RHA-SO_3H.

slit-like pores [33]. These results also prove that the textural properties of RHA were substantially maintained over sulfonic acid functionalization. Table 2 shows the specific BET surface areas, pore volumes and pore diameters for RHA and RHA-SO_3H. A decrease in the surface area was observed for RHA and RHA-SO_3H from 57 to 40 m^2/g, respectively. This suggests that sulfonic acid may be well confined in the pores of RHA, and indicates an ordered mesoporosity of the support even after modification. The curves of pore size distribution evaluated from desorption data by utilizing the BJH model are also shown in Fig. 4b.

3.1.5. SEM analysis

The samples of RHA and RHA-SO_3H were analyzed by scanning electron microscopy (SEM), as represented in Fig. 5. The pictures show that RHA has a porous and irregular shape, thus its high specific surface area can be explained [31]. These images also show that the primary morphology of RHA is changed after modification with chlorosulfonic acid. Indeed, the comparison of the RHA and RHA-SO_3H indicated that the particles are aggregated after modification.

Table 2
Pore structure parameters of RHA and RHA-SO_3H derived from the N_2 adsorption–desorption isotherms.

Sample	S_{BET} (m^2/g)	V_{BJH} (cm^3/g)	D_{BJH} (nm)
RHA	57	0.19	10.4
RHA-SO_3H	40	0.16	11.6

3.1.6. pH analysis of catalyst

To 25 mL of an aqueous solution of NaCl (1 M) with a primary pH 5.2, RHA-SO_3H (0.5 g) was added and the resulting mixture was stirred for 2 h at room temperature after which the pH of solution decreased to 1.3. This is equal to a loading of 2.5 mmol H^+/g [34].

3.1.7. Hammett acidity

The Hammett acidity method is an effective way to measure the acidity strength of an acid in organic solvents, using UV–vis technique [35]. The Hammett function is defined as:

$$H_0 = pK(\mathrm{I})_{aq} + \log\left([\mathrm{I}]_s / \left[\mathrm{IH}^+\right]_s\right).$$

Where the $pK(\mathrm{I})_{aq}$ is the pK_a value of aqueous solution of indicator, and $[\mathrm{IH}^+]_s$ and $[\mathrm{I}]_s$ are the molar concentrations of protonated and unprotonated forms of the indicator in the solvent, respectively. According to Lambert–Beer's Law, the value of $[\mathrm{I}]_s/[\mathrm{IH}^+]_s$ can be determined and calculated through UV–visible spectrum.

For this purpose, 4-nitroaniline ($pK(\mathrm{I})aq = 0.99$) as the basic indicator and CCl_4 as the solvent were chosen. As can be seen in Fig. 6, the maximal absorbance of the unprotonated form of the indicator was observed at 329 nm in CCl_4. When RHA-SO_3H as a solid acid catalyst was added to the indicator solution, the absorbance of the unprotonated form of the indicator decreased, which indicated that the indicator was partially in the form of $[\mathrm{IH}^+]$. These results listed in Table 3, show the acidity strength of RHA-SO_3H.

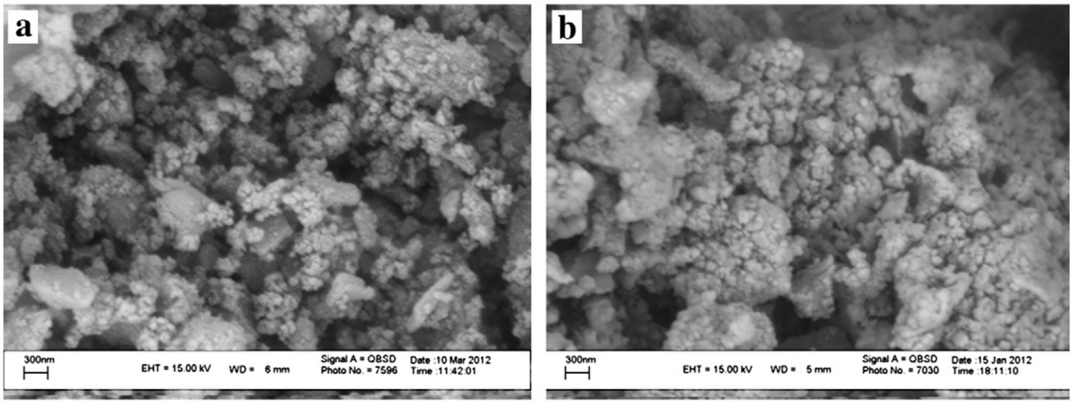

Fig. 5. SEM images of (a) RHA and (b) RHA-SO_3H, respectively.

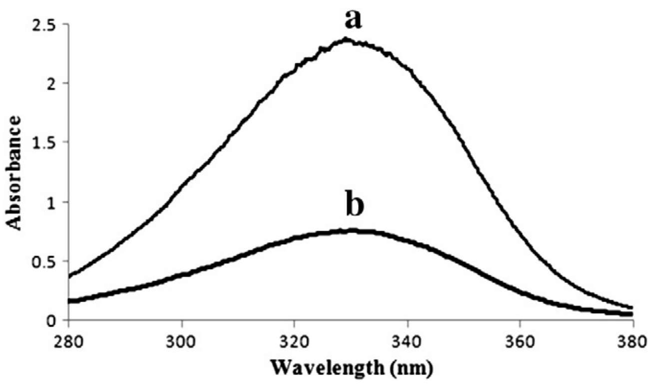

Fig. 6. Absorption spectra of 4-nitroaniline (indicator) (a) and RHA-SO_3H (catalyst) (b) in CCl_4.

Table 3
Calculation of Hammett acidity function (H_0) for RHA-SO_3H.

Entry	Catalyst	A_{max}	$[I]_s$ %	$[IH^+]_s$ %	H_0
1	–	2.3803	100	0	–
2	RHA-SO_3H	0.7549	31.71	68.29	0.65

Condition for UV–visible spectrum measurement: solvent: CCl_4, indicator: 4-nitroaniline ($pK(I)_{aq} = 0.99$), 1.44×10^{-4} mol/L; Catalyst: RHA-SO_3H, 20 mg, 25 °C.

3.3. Catalytic activity

On the basis of the information obtained from the above mentioned studies, we anticipated that RHA-SO_3H can be used as an efficient catalyst for the promotion of the reactions which need the use of an acidic catalyst to speed up. So we were interested to investigate the applicability of the reagent in the acetylation of aldehydes using acetic anhydride.

For optimization of the reaction conditions, conversion of 4-chlorobenzaldehyde with acetic anhydride to its corresponding 1,1-diacetate was chosen as a model reaction and the various conditions including amount of the catalyst and acetic anhydride, solvent and temperature were examined. Finally the optimal reaction condition for this reaction was as follows: 1 mmol aldehyde, 1.5 mmol acetic anhydride and 10 mg RHA-SO_3H as catalyst at room temperature and solvent free condition, as shown in Scheme 2. The preparation of 1,1-diacetate from 4-chlorobenzaldehyde was also carried out in the absence of the catalyst and in the presence of rice husk ash but the reactions did not proceed even after 1 h. These results indicated that the catalyst is necessary to produce the products. Any further increase in the amount of the catalyst or temperature did not improve the reaction time and yield.

To reveal the generality of this method, we next explored the protocol with a variety of aromatic, aliphatic and heterocyclic aldehydes under the optimal conditions. The results were presented in Table 4. It was observed that under similar conditions, a wide range of aromatic aldehydes containing electron-withdrawing as well as electron-donating groups such as Cl, Br, F, CH_3, OCH_3 and NO_2 is easily protected with acetic anhydride in short reaction times with good to excellent isolated yields (Table 4, entries 1–14). It should be noted that the reaction conditions were mild enough to induce any damage to the acid sensitive moieties like methoxy group (Table 4, entries 10–12) and acid-sensitive substrates like furfural (Table 4, entry 15). When the reaction was extended towards hydroxybenzaldehydes, the hydroxyl groups were also protected as acetates. In these cases higher amount of catalyst was needed due to the strong electron donation of OH group and high steric hindrance (Table 4, entries 16–17).

Cinnamaldehyde, as an α,β-unsaturated aldehyde, was also acetylated in high yield using this procedure without the isomerization of double bond (Table 4, entry 18). Furthermore, polycyclic aromatic aldehydes such as 2-naphthaldehyde and fluorene-3-carbaldehyde also provided the desired acylals in very good yields (Table 4, entries 19–20). This method was also found to be useful for the protection of benzenedicarbaldehydes, phthaldialdehyde and terephthaldialdehyde, that gave the tetraacetylated products in good yield (Table 4, entries 21–22). Furthermore, using this method pentanal as an aliphatic aldehyde was also converted to its corresponding acylal in high yields at ambient temperature and under solvent-free condition (Table 4, entry 23).

Dimethylaminobenzaldehyde failed to give the corresponding 1,1-diacetates which may be due to the electron-donating of dimethylamino group (Table 4, entry 24).

To evaluate the chemoselectivity of the method we also investigated the acylation of ketones. Under this catalytic system, acylation of acetophenone was not successful and no product was obtained (Table 4, entries 25–26). This observation indicates the chemoselectivity of the protocol and that aldehydes are more reactive than ketones due to higher electrophilicity of aldehyde in comparison to ketones.

Also we investigated the application of RHA-SO_3H as catalyst for deprotection of acylals to their corresponding aldehydes. For this purpose, the acylals were treated with 30 mg of catalyst in acetonitrile at 60 °C. In this condition, the corresponding aldehydes were obtained in good to high yields, as results are summarized in Table 3. We found that nitro derivatives (Table 4, entries 13–14) gave lower yields (<50%) in acetonitrile after 1 h, whereas in refluxing toluene they were quantitatively deprotected after 5 min. This may be due to the strong electron-withdrawing effect of the nitro substituent, which requires a high refluxing temperature.

To check the reusability of the catalyst, the reaction of 4-chlorobenzaldehyde and acetic anhydride under the optimized reaction conditions was studied again. When the reaction completed, dichloromethane was added and the catalyst was separated by filtration. The recovered catalyst was washed with dichloromethane, dried and reused for the same reaction. This process was carried out over three runs and all reactions were led to the desired products without any changes in terms of the reaction time and yield which clearly demonstrates practical recyclability of RHA-SO_3H. Further pH analysis of the recovered catalyst showed loading of 2.4 mmol H^+/g. This result suggests that the nature of the catalyst remains intact after each run and leaching of the acid species did not occur during the course of the reaction.

In order to show the efficiency of the present method, we have compared our results obtained from the acetylation of 4-chlorobenzaldehyde with acetic anhydride catalyzed by RHA-SO_3H with other results reported in the literature. As can be seen in Table 5, this method avoids disadvantages of other procedure such as long reaction times, low yields and excess reagents. This comparison also clarifies an important point about the catalyst. As it can be seen $FeCl_3$, Al_2O_3 and P_2O_5 are also able to catalyze this type of reactions, but in higher amounts than there are in RHA-SO_3H. As reported in the literature, 100 mg of $FeCl_3$ and 50 mg of P_2O_5/Al_2O_3 are needed for the promotion of the acetylation of aldehydes (Table 5, entries 1 and 4), while the available amounts of Fe, Al and P in RHA are 0.38, 0.25 and 0.44 wt.%, respectively. So their concentration in the catalyst is very low and is

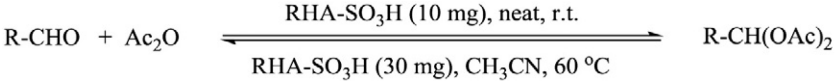

$$\text{R-CHO} + \text{Ac}_2\text{O} \underset{\text{RHA-SO}_3\text{H (30 mg), CH}_3\text{CN, 60 °C}}{\overset{\text{RHA-SO}_3\text{H (10 mg), neat, r.t.}}{\rightleftharpoons}} \text{R-CH(OAc)}_2$$

Scheme 2. The protection and deprotection of aldehydes catalyzed by RHA-SO_3H.

Table 4
Acylation of aldehydes and deprotection of acylals catalyzed by RHA-SO_3H.

Entry	Substrate	Product	Protection				Deprotection	
			Time (min)	Yield (%)	m.p. (°C)		Time (min)	Yield (%)
					Found	Reported		
1	C_6H_5CHO	$C_6H_5CH(OAc)_2$	0.5	94	43–45	43–44 [16]	4	91
2	2-ClC_6H_4CHO	2-$ClC_6H_5CH(OAc)_2$	0.5	93	57–59	58–60 [17]	5	92
3	3-ClC_6H_4CHO	3-$ClC_6H_5CH(OAc)_2$	0.5	92	66–68	64–65 [15]	4	89
4	4-ClC_6H_4CHO	4-$ClC_6H_5CH(OAc)_2$	0.5	95	82–84	81–83 [16]	4	92
5	3-BrC_6H_4CHO	3-$BrC_6H_5CH(OAc)_2$	0.5	90	72–74	83 [12]	5	88
6	4-BrC_6H_4CHO	4-$BrC_6H_5CH(OAc)_2$	0.5	97	81–83	84 [12]	4	94
7	4-FC_6H_4CHO	4-$FC_6H_5CH(OAc)_2$	0.5	96	52–54	51–53 [17]	3	95
8	2-$CH_3C_6H_5CHO$	2-$CH_3C_6H_5CH(OAc)_2$	0.5	93	64–66	65–67 [19]	3	90
9	3-$CH_3C_6H_5CHO$	3-$CH_3C_6H_5CH(OAc)_2$	0.5	93	Oil	Oil [12]	2	91
10	2-$CH_3OC_6H_5CHO$	2-$CH_3OC_6H_5CH(OAc)_2$	0.5	89	75–77	73–74 [15]	3	90
11	3-$CH_3OC_6H_5CHO$	3-$CH_3OC_6H_5CH(OAc)_2$	0.5	95	Oil	Oil [15]	3	92
12	4-$CH_3OC_6H_5CHO$	4-$CH_3OC_6H_5CH(OAc)_2$	0.5	83	61–63	64–65 [16]	4	94
13	3-$NO_2C_6H_4CHO$	3-$NO_2C_6H_4CH(OAc)_2$	0.5	95	66–68	65–67 [15]	5	87[a]
14	4-$NO_2C_6H_4CHO$	4-$NO_2C_6H_4CH(OAc)_2$	0.5	93	124–126	124–126 [15]	5	89[a]
15	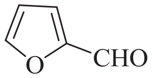	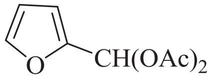	0.5	87	52–54	52–53 [15]	1	94
16[b,c]	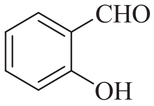	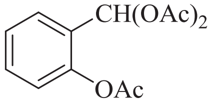	1	90	101–103	101–102 [15]	5	93[b,c]
17[c,d]	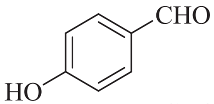	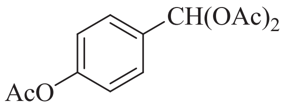	1.5	94	91–93	90–92 [15]	5	94[c,d]
18	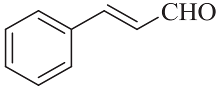	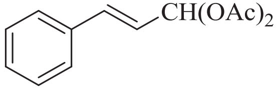	1	91	83–85	84–86 [15]	2	92
19	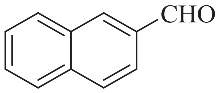	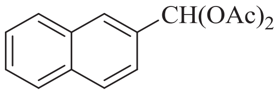	0.5	93	102–104	101 [12]	5	90
20	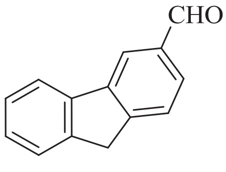	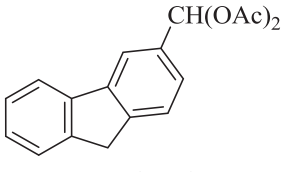	0.5	92	130–132	–	1	91
21[c]	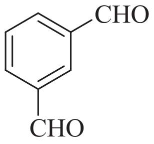	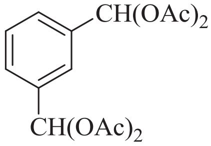	2.5	89	100–102	96–98 [19]	10[d]	87[c,e]
22[c]	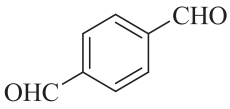	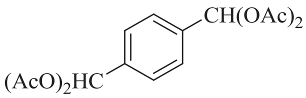	1.5	90	172–174	172–174 [17]	8[d]	89[c,e]
23	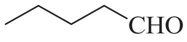	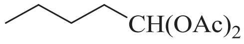	1	91	Oil	Oil [15]	5	88
24	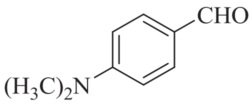	–	1 h	0	–	–	–	–
25	$C_6H_5COCH_3$	–	1 h	0	–	–	–	–
26	C_6H_5CHO + $C_6H_5COCH_3$	$C_6H_5CH(OAc)_2$ + –	0.5	100 + –				

[a] The reaction was performed in refluxing toluene.
[b] 20 mg of the catalyst was used.
[c] 3 mmol acetic anhydride was used.
[d] 50 mg of the catalyst was used.
[e] 60 mg of the catalyst was used.

Table 5
Comparison of the results of the acylation of benzyl alcohol catalyzed by RHA-SO_3H with those obtained by some of the other reported catalysts.

Entry	Catalyst	Catalyst loading	Reaction conditions	Time (min)	Yield (%)	Ref.
1	$FeCl_3$	100 mg	0 °C/neat	35	79	[2]
2	Zn-montmorillonite	2 g	r.t./neat	24 h	99	[6]
3	$In(OTf)_3$	0.1 mol%	r.t./CH_2Cl_2	5	95	[8]
4	P_2O_5/Al_2O_3	100 mg	r.t./neat	45	86	[9]
5	$CuSO_4.5H_2O$	5 mol%	r.t./neat	15	99	[10]
6	Silica Sulfuric Acid	200 mg	r.t./neat	30	84	[11]
7	$HClO_4$-SiO_2	50 mg	r.t./neat	2	97	[12]
8	$Al(HSO_4)_3$	43 mg	r.t./neat	5	75	[13]
9	SO_4^{2-}/SnO_2	15 mg	r.t./neat	25	90	[14]
10	[Hmim]HSO_4	3.8 mol%	r.t./neat	25	90	[15]
11	[bmpy]HSO_4	10 mol%	r.t./US	5	97	[16]
12	silica-bonded S-sulfonic acid	5 mg	r.t./neat	4	84	[17]
13	saccharin sulfonic acid	50 mg	r.t./neat	50	90	[18]
14	ZSM-5-SO_3H	20 mg	r.t./neat	1	95	[20]
	ZSM-5-SO_3H	20 mg	r.t./CH_2Cl_2	4	50	[20]
15	RHA-SO_3H	10 mg	r.t./neat	0.5	94	This work

not enough to promote the requested reactions. It is also important to note that among the reported catalysts the activity and amount of ZSM-5-SO_3H are near to RHA-SO_3H. In spite of this similarity the difference is that the ZSM-5 zeolite was synthesized using various chemical compounds such as hydrated aluminum sulfate, tetrapropylammonium bromide, sodium silicate solution and sodium chloride and at high temperatures (110, 230, 540 °C) during a long time (24 h) while RHA can be prepared from an agricultural residue using a simple experimental method.

4. Conclusion

In conclusion, in the study we have introduced RHA-SO_3H a highly powerful solid acid catalyst for the simple, efficient and chemoselective acylation of various aldehydes and deprotection of the obtained 1,1-diacetates. All reactions are carried out in very short reaction time. Furthermore, the methodology has several advantages such as high reaction rates, no side reactions, ease of preparation and handling of the catalyst, simple experimental procedure, cleaner reactions, use of inexpensive and reusable catalyst with lower loading and solvent free conditions. Further studies on some more practical applications of the RHA-SO_3H catalyst in other organic reactions are currently underway in our laboratory.

Acknowledgments

We are thankful to the University of Guilan Research Council for the partial support of this work.

References

[1] T.W. Greene, P.G.M. Wuts, Protective Groups in Organic Synthesis, third ed., John Wiley and Son Inc., New York, 1999, pp. 306–307.
[2] K.S. Kochhar, B.S. Bal, R.P. Deshpande, S.N. Rajadhyaksha, H.W. Pinnick, Journal of Organic Chemistry 48 (1983) 1765–1767.
[3] M. Sandberg, L.K. Sydnes, Tetrahedron Letters 39 (1998) 6361–6364.
[4] J.G. Frick, R.J. Harper, Journal of Applied Polymer Science 29 (1984) 1433–1447.
[5] M.J. Gregory, Journal of the Chemical Society B: Physical Organic (1970) 1201–1207.
[6] N.M. Nagy, M.A. Jakab, J. Konya, S. Antus, Applied Clay Science 21 (2002) 213–216.
[7] D.H. Aggen, J.N. Arnold, P.D. Hayes, N.J. Smoter, R.S. Mohan, Tetrahedron 60 (2004) 3675–3679.
[8] R. Ghosh, S. Maiti, A. Chakraborty, R. Halder, Journal of Molecular Catalysis A: Chemical 215 (2004) 49–53.
[9] A.R. Hajipour, A. Zarei, A.E. Ruoho, Tetrahedron Letters 48 (2007) 2881–2884.
[10] M.M. Heravi, S. Taheri, K. Bakhtiari, H.A. Oskooie, Monatshefte fur Chemie 137 (2006) 1075–1078.
[11] U.V. Desai, T.S. Thopate, D.M. Pore, P.P. Wadgaonkar, Catalysis Communications 7 (2006) 508–511.
[12] A.T. Khan, L.H. Choudhury, S. Ghosh, Journal of Molecular Catalysis A: Chemical 255 (2006) 230–235.
[13] B.F. Mirjalili, M.A. Zolfigol, A. Bamoniri, M.A. Amrollahi, N. Sheikhan, Russian Journal of Organic Chemistry 43 (2007) 852–854.
[14] J.R. Satam, R.V. Jayaram, Catalysis Communications 8 (2007) 1414–1420.
[15] A.R. Hajipour, L. Khazdooz, A.E. Ruoho, Catalysis Communications 9 (2008) 89–96.
[16] S.P. Borikar, T. Daniel, Ultrasonics Sonochemistry 18 (2011) 928–931.
[17] K. Niknam, D. Saberi, M. NouriSefat, Tetrahedron Letters 50 (2009) 4058–4062.
[18] F. Shirini, M. Mamaghani, T. Mostashari-Rad, M. Abedini, Bulletin of the Korean Chemical Society 31 (2010) 2399–2401.
[19] F. Shirini, O.G. Jolodar, Journal of Molecular Catalysis A: Chemical 356 (2012) 61–69.
[20] A.R. Massah, R.J. Kalbasi, A. Shafiei, Monatshefte fur Chemie 143 (2012) 643–652.
[21] S. Chakraborty, S. Chowdhury, P.D. Saha, Carbohydrate Polymers 86 (2011) 1533.
[22] D.B. Martin, Energy From Rice Residues, Winrock international, Arlington, USA, 1990.
[23] C. Real, M.D. Alcalá, J.M. Criado, Journal of the American Ceramic Society 79 (1996) 2012–2016.
[24] Q. Feng, H. Yamamichi, M. Shoya, S. Sugita, Cement and Concrete Research 34 (2004) 521–526.
[25] P. Chindaprasirt, C. Jaturapitakkul, U. Rattanasak, Fuel 88 (2009) 158–162.
[26] H. Chao-Lung, B.L. Anh-Tuan, C. Chun-Tsun, Construction and Building Materials 25 (2011) 3768–3772.
[27] V.C. Srivastava, I.D. Mall, I.M. Mishra, Colloids and Surfaces A: Physicochemical and Engineering Aspects 312 (2008) 172–184.
[28] M.C. Manique, C.S. Faccini, B. Onorevoli, E.V. Benvenutti, E.B. Caramão, Fuel 92 (2012) 56–61.
[29] D. An, Y. Guo, Y. Zhu, Z. Wang, Chemical Engineering Journal 162 (2010) 509–514.
[30] H.R. Shaterian, M. Ghashang, M. Feyzi, Applied Catalysis A: General 345 (2008) 128–133.
[31] G.A. Habeeb, H.B. Mahmud, Materials Research 13 (2010) 185–190.
[32] F. Shirini, M. Mamaghani, S.V. Atghia, Catalysis Communications 12 (2011) 1088–1094.
[33] J.B. Condon, Surface Area and Porosity Determinations by Physisorption, Elsevier, 2006. (Chapter 1, pp. 1-27).
[34] D. Zareyee, B. Karimi, Tetrahedron Letters 48 (2007) 1277–1280.
[35] H. Xing, T. Wang, Z. Zhou, Y. Dai, Journal of Molecular Catalysis A: Chemical 264 (2007) 53–59.